Separation and Purification Technology 325 (2023) 124535

Contents lists available at ScienceDirect

Separation and Purification Technology

journal homepage: www.elsevier.com/locate/seppur

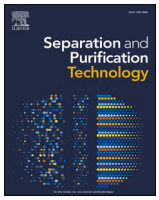

Chitosan-based mixed matrix composite membranes for CO_2/CH_4 mixed gas separation. Experimental characterization and performance validation

Andrea Torre-Celeizabal [a], Clara Casado-Coterillo [a,*], Alicia Gomis-Berenguer [b], Jesús Iniesta [b], Aurora Garea [a]

[a] Department of Chemical and Biomolecular Engineering, Universidad de Cantabria, Av. Los Castros s/n, 39005, Santander, Spain
[b] Department of Physical Chemistry, Institute of Electrochemistry, Universidad de Alicante, Av. Raspeig s/n, 03080, Alicante, Spain

ARTICLE INFO

Keywords:
Chitosan biopolymer-based membranes
Na^+-containing microporous fillers
Membranes characterization
CO_2 permeance
validation of CO_2/CH_4 mixture separation

ABSTRACT

Membrane technology is acknowledged as one of the most efficient for biogas upgrading, separating simultaneously CH_4 and CO_2 in the retentate and permeate streams, respectively. The sustainability would still be improved by using renewable and environmentally friendly materials for membrane fabrication. Specifically, this study is focused on laboratory-scale mixed gas separation tests of composite membranes prepared from chitosan (CS), a hydrophilic, biodegradable and biocompatible polymer from abundant natural resources, with good adhesive and film forming properties and high affinity for CO_2 due to the primary amine and hydroxyl groups functionalities in CS. To improve mechanical resistance and CO_2/CH_4 separation, CS was hybridized by a 5 wt% loading of non-toxic ionic [emim][acetate] liquid (IL), and variable loadings of compatible inorganic fillers, such as 3D zeolite 4A and NaETS-10, and layered AM-4 titanosilicate. The CS-based mixed matrix layer was coated on porous polyether sulfone (PES) support. The CO_2 permeance and CO_2/CH_4 separation were measured at different feed concentrations to evaluate the membranes performance in the treatment of different streams. This separation behavior was explained by the wet thickness, water uptake, morphology and ionic resistance of the composite membrane. As such, the 5 wt% Zeolite 4A and NaETS-10-filled ILCS/PES membranes provided a good dispersion in the ILCS matrix and the mixed matrix layer a good adhesion with the porous PES support, leading to high CO_2 permeances and separation factors up to 30, whereas the more hydrophilic lamellar AM-4 titanosilicate-filled ILCS layer showed cluster agglomeration in the matrix and a faster detachment of the coated layer from the PES substrate. With increasing filler loading, an increase of the permeance of both CO_2 and CH_4 gas components was, although selectivity decreased upon increasing AM-4 filler loading. The CO_2/CH_4 mixed gas separation performance was validated by a custom-built model for a wide range of feed composition, to cover such processes as natural gas sweetening, biogas upgrading and enhanced oil recovery with acceptable relative error below 10% (absolute value), except for the AM-4 titanosilicate-filled ILCS membranes, showing morphological fabrication defects.

1. Introduction

The devastating effects of climate change have led governments to determine different strategies, leading to the introduction of environmental regulations to promote the use of renewable forms of energy to decarbonize the economy [1]. To address this challenge, biogas could be used for energy production in order to obtain biomethane as power source for which it is crucial the separation of CH_4 from CO_2. Although membrane technology is acknowledged as one of the efficient tools for biogas upgrading due to advantages such as small footprint, low-cost, high-energy efficiency, easy processability and handling, the sustainability of the fabrication can still be improved by using renewable and environmentally friendly materials. The outcome of circular economy and decarbonization has thus attired the focus on the potential of biopolymers and materials from renewable sources as a means of sustainable fabrication of membranes with functionalities at least as good as those of conventional fossil-based polymers. In this regard, several reviews have appeared in the last couple of years [2–5].

In this regard, new sustainable routes for gas separation membranes are being open by the application of less toxic solvents [6–8] and the

* Corresponding author.
E-mail address: casadoc@unican.es (C. Casado-Coterillo).

https://doi.org/10.1016/j.seppur.2023.124535
Received 20 March 2023; Received in revised form 1 June 2023; Accepted 6 July 2023
Available online 16 July 2023

substitution of chemically synthesized polymers by biopolymers [2,9–11]. Biopolymers are defined as polymers coming from renewable sources or biodegradable polymers after their use, thus their interest because they do not take place in landfills and may represent a worthy alternative to traditional fossil fuel-based polymers. In this aspect, biopolymers reported for membrane preparation are usually chitosan (CS) [3], cellulose acetate (CA) [4], poly-lactic acid (PLA) [12], polyurethane (PU) [13], poly vinyl alcohol (PVA) [14], starch [15] and in lesser way, polyhydroxybutyrate (PHBs) [8]. They all come from different sources, and they present different degrees of hydrophilicity, mechanical robustness and biodegradability, so they are very difficult to classify. Recent review papers collect the properties of most common bio-based materials [10].

CA membranes have been known for quite a while in biogas upgrading [4], among other polysaccharides. Among them, CS is of particular interest, being a non-toxic, hydrophilic, multi-functional, biodegradable and biocompatible polymer from abundant natural resources, with good adhesive and film forming properties [3,16]. Its high affinity for CO_2 is linked to the primary amine and hydroxyl functional groups, which is reinforced in humid conditions [17–19]. The presence of water in hydrophilic biopolymers, like PU [20], CS and starch, facilitates the transport of CO_2 through the membrane, in addition to the solution-diffusion mechanism common in polymer based materials [21]. The biopolymer capability of increasing CO_2 permeability in wet conditions, which seemed to be improved in water-swollen state, has been studied on the modification of composite membranes for CO_2/CH_4 separation, like Pebax/PES [22]. Other polymers that are usually encountered under the 'biopolymer' classification in literature are those obtained from wastes, like silk-fibroin [23]. The chemical grafting of cellulose acetate membranes originally produced for reverse osmosis and nanofiltration have shown potential on biogas upgrading [24].

CO_2-rich residual streams contain water vapor that needs to be removed before conventional capture processes. However, CS biopolymer membranes improve their CO_2 permeance and CO_2/CH_4 separation abilities in wet conditions [17,25,26]. The blending of other waste-based biopolymer with CS improves the CO_2 separation in humid conditions as most of CO_2-containing effluent streams are [18]. Common properties in biopolymers are a high hydrophilicity and low to moderate mechanical strength, both parameters influencing the transport of gases, such as CO_2, and the durability of the membrane for an acceptable lifetime [21]. Both the CO_2 affinity and mechanical properties of chitosan, as other polymers, can be improved by adding small loadings of 1-ethyl-4-methyl imidazolium acetate ionic liquid (IL), and zeolite-based three dimensional and two-dimensional particles [27–31] in the form of a mixed matrix membrane (MMM).

Spectroscopic techniques are relatively common in order to determine the structural–functional relationship in MMM. Jomeikian et al. used ^{13}C NMR spectroscopy to observe the C–C interactions between the grafted gC_3N_4 employed in order to prevent the agglomeration of ZIF-8 particles within the CS matrix and improve the CO_2/CH_4 separation performance [32]. These techniques may as well provide insight into the fabrication of gas separation membranes from biopolymers, with ion exchange capacity and hydrophilicity of similar values of ion exchange membranes.

The relationship between membrane materials properties and the separation performance necessary to optimize the membrane operation is usually limited to the use of the Robeson upper bound and single permeability and selectivity values [33,34]. The correlation of physicochemical properties with the functional transport characterization [2,5,6] can provide insightful information for the reliability of biopolymer based membrane performance in fields such as CO_2/CH_4 separation. In order to overcome the trade-off between transport and mechanical resistance, a common challenge in hydrophilic biopolymers, it is necessary to establish the quantitative properties-function relationship enabling prediction of new sustainable membrane materials in gas separation membranes [35].

In a previous work, we presented a cross-flow mathematical model predicting the CO_2/CH_4 separation performance of composite ionic liquid blended chitosan membranes on porous polyether sulfone (PES) support and a commercial silicon rubber membrane based on pure gas permeation experiments [36]. This work continues that research line, by including the analysis of mixed gas separation performance of the CS-based mixed matrix composite membranes coated on compatible PES porous support, varying the feed concentration and composition of the selective layer. To form this layer, CS was hybridized with the non-toxic [emim][acetate] ionic liquid (IL), and different inorganic fillers prepared with non-critical inorganic reactants and no costly organic surfactants, whose compatibility with the CS biopolymer matrix and CO_2 preferential solubility towards CH_4 [28,37] was proven in previous studies [29], before being coated on a porous PES support [38,39]. The CO_2 permeance and CO_2/CH_4 mixture selectivity were measured at different feed compositions in order to address different processes. The structure–function relationship was evaluated by analyzing the transport and separation performance in the light of the water uptake, swelling degree, attenuated total multiple reflection Fourier transformed IR (ATR-FTIR), Electrochemical Impedance Spectroscopy (EIS) and scanning electron microscopy (SEM) observations of the selective membrane layer. The results were validated with the process simulation model previously developed in our group [36,40].

2. Experimental section

2.1. Materials

The main polymer used for the thin selective layer fabrication was chitosan biopolymer (Sigma Aldrich, Spain). Trimesoyl chloride (TMC) solution in hexane (Sigma Aldrich, Spain) was used to treat the surface of the polyether sulfone (PES) porous support (0.1 μm pore size, PALL, Micromeritics, Spain) prior to the coating of the hydrophilic biopolymer-based layer. The commercial fillers used in this work were Zeolite 4A (Fluka, Sigma Aldrich, Spain), and 1-Ethyl-3-methylimidazolium acetate [emim][Ac] ionic liquid (Sigma Aldrich, Spain).

2.2. Membrane preparation

Flat-sheet composite MMMs were prepared in our laboratory by a modification of the interfacial polymerization process. A commercial PES porous disk was used as support because of its favorable characteristics such as wide operating temperature, broad pH limit, low cost, good chemical and mechanical resistance and easy to be fabricated into different geometries, which make it an excellent option as a support [41]. Firstly, the surface of the PES commercial membrane was treated with a hydrophobic solution of 0.1 wt% TMC/hexane at 50 °C in order to avoid the penetration and crystallization of the hydrophilic semi-crystalline chitosan in the opening of the PES pores [39,42]. The top selective layer consists of a solution of 1 w/v% CS biopolymer in 2 wt% acetic acid/H_2O, to which IL was added up to a 5 wt% of the total polymer weight, as optimized previously in our research group [39]. In order to prepare the mixed matrix composite membranes, different types of Na^+-containing porous inorganic fillers were used to improve the performance of the biopolymer-based coating: 3D Zeolite 4A [37] and ETS-10 titanosilicate [28] and 2D AM-4 titanosilicate [36]. Lamellar AM-4 and 3D ETS-10 titanosilicate nanoparticles were prepared by hydrothermal synthesis without organic surfactant-directing structural agents as reported elsewhere [43,44]. The fillers were dispersed in 2 mL water before being added to the IL-CS solution, as a 5 and 10 wt% loading of the total polymer matrix. Membranes were finally neutralized by immersion in NaOH 1 M for 1 h and thorough rinsing with ultrapure water, to eliminate the excess of NaOH, in order to charge the membrane with OH^- ionic groups and increase its affinity towards CO_2 before gas separation and characterization experiments.

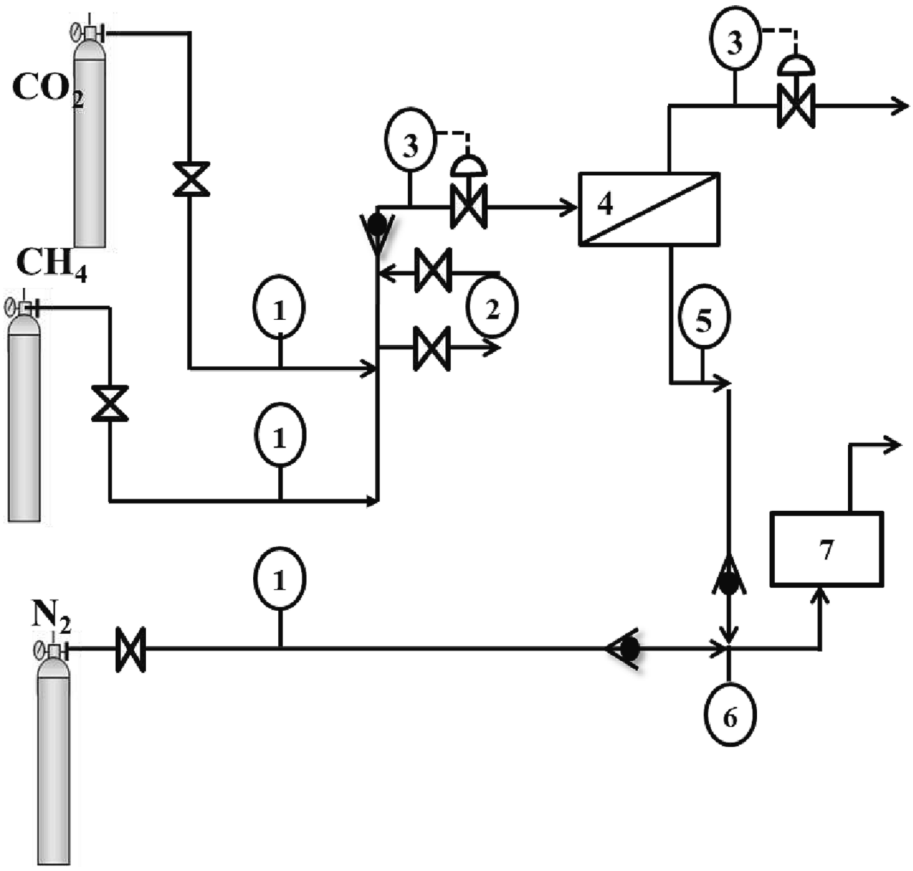

Fig. 1. Scheme of the experimental setup [36]. (1) Mass flow controller; (2) water bubbler; (3) feed and retentate pressure regulator; (4) membrane module; (5) permeate pressure indicator; (6) permeate flowmeter; (7) permeate gas composition analyzer.

2.3. Characterization

Membrane thickness was measured using a digital micrometer (IP-65 digimatic micrometer, Mitutoyo, Japan) with an accuracy of 0.001 mm. Four points of the effective area of the membrane were measured and the average thickness and standard deviation were calculated. Swelling Degree (SD) was determined using equation (1) by measuring membrane thickness before, t_{wet} and after, t_{dry}, gas permeation experiments.

$$SD(\%) = \frac{t_{wet} - t_{dry}}{t_{dry}} \times 100 \quad (1)$$

The wet weight was obtained by quickly blotting the membrane on tissue paper to remove the excess water and the dry weight was measured after the gas permeation experiments. This allows to obtain the Water Uptake (WU) as

$$\mathrm{WU}(\%) = \frac{W_{wet} - W_{dry}}{W_{dry}} \times 100 \quad (2)$$

ATR-FTIR spectroscopy was conducted using a Perkin Elmer spectrometer to study the chemical composition by analyzing the functional groups and interactions in the membranes surface of the different mixed matrix composite membranes after the permeation experiments. The spectrum used in the study was taken over 4 scans at a wave number resolution of 4 cm^{-1} in the range 400–4000 cm^{-1}.

EIS was measured in a 2-electrode electrochemical cell for all membranes in order to correlate the resistance of the selective membrane layer with the diffusional physical–chemical properties. EIS experiments were performed using a Bio-logic system equipment equipped with an impedance module in a potentiostatic method. The alkaline activated membrane was placed between smooth stainless steel-plated electrodes with a projected geometric area of 1.13 cm^2. The cell was subjected to a constant pressure until the Nyquist plot was repeatedly the same. The amplitude was set at 10 mV (7.0 mV rms) and the frequency range was varied between 1.0 MHz and 0.1 Hz. Measurements were repeated for reproducibility verification.

Cross-sectional area and morphology of selected membranes of each composition of the selective layer were observed by scanning electron microscopy (SEM) in a JSM-IT2500 HR (JEOL) microscope. Samples were prepared by freezing in liquid nitrogen before being fractured with a sharp cut from a freshly sharpened blade and sputtering with silver prior to observation. This enabled to observe whether the membrane thickness agreed with the one measured to determine the quality of the coating. This technique also allowed us to check the distribution as well as the homogeneity of the coating and the interaction between the polymer matrix and the fillers through the surface area images.

2.4. Gas separation experiments

A stainless-steel module with an effective membrane area of 15.6 cm^2 was used for the characterization of the permeability of the membranes prepared in this work. It consists of two stainless steel pieces with a cavity where the membrane is placed onto a 316LSS microporous disk support with a pore size of 20 μm and sealed by Viton rings. Different feed mixture concentrations of CH_4 and CO_2 were used in order to focus on different processes, such as natural gas sweetening, biogas upgrading or enhanced oil recovery, from low to high concentration of CO_2 in the feed. Feed mixtures of CO_2:CH_4 were introduced to the system in concentration relationships of 20:80, 35:65, 50:50, and 70:30 v/v%, respectively.

The experiments were carried out with the home-made separation plant represented in Fig. 1. The feed pressure in all the experiments was set at 4 bar. The total feed flow rate was set in all cases to 50 mL/min and

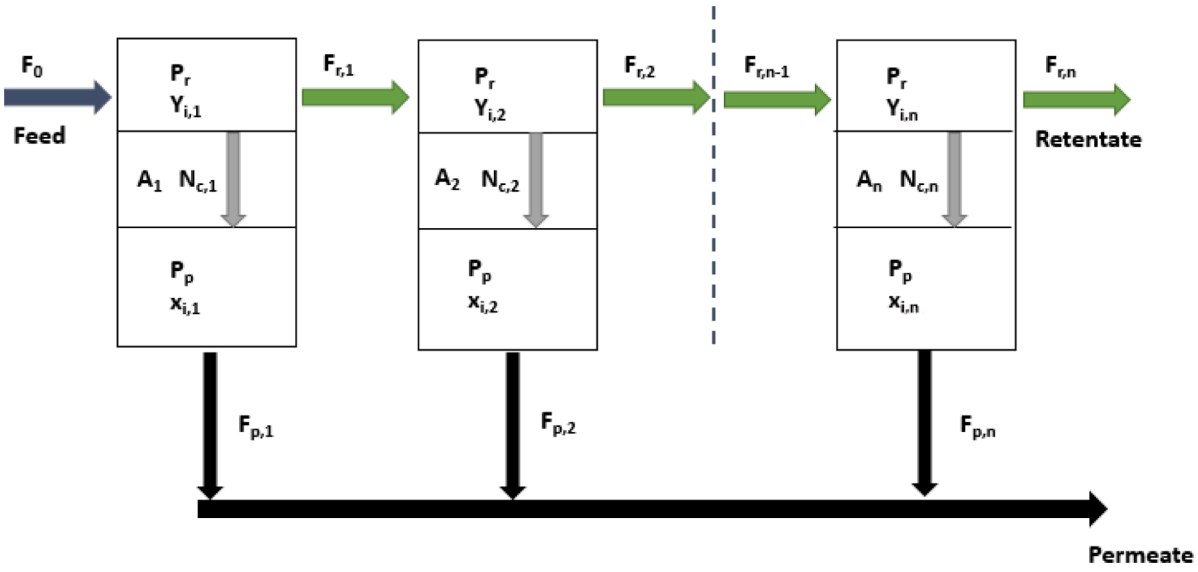

Fig. 2. Diagram of the cross-flow membrane model ().
adapted from [36]

gas mass flow controllers (KOFLOC 8500, Sequopro S.L., Madrid, Spain) were used to establish the desired quantity of each gas component. The permeate flowrate was measured with a bubble flowmeter, before deriving the stream to a BIOGAS 5000 gas analyzer (Geotech Tamarac, FL, USA) in order to quantify the composition of the permeate flowrate. Permeation experiments were performed until the system reached the steady state. After two series of experiments at a different feed concentration, the feed stream was humidified by passing 50% through a water bubbler for 1 h during conditioning at the following concentration point, before sampling data measurements to ensure that the membrane was maintained at constant WU values over the whole experimental run to avoid the usual drop of flux observed when hydrophilic biopolymer-based membranes dried.

The permeance of the gas (1 GPU = 10^{-6} cm^3 (STP) cm^{-2} s^{-1} $cmHg^{-1}$) is defined as the pressure-normalized flux of a gas through a membrane,

$$\left(\frac{P}{t}\right)_i = \frac{F_p y_i}{(p_r x_i - p_p y_i)A} x10^6 \tag{3}$$

where P is the intrinsic permeability of the desired component on the selective membrane layer in Barrer (1 Barrer = 10^{-10} cm^3 (STP) cm cm^{-2} s^{-1} $cmHg^{-1}$); p_p and p_r are the permeate and retentate pressures, in cmHg, respectively; A is the effective membrane area for permeation (cm^2); t is the selective layer thickness (cm); F_p is the permeate flowrate (cm^3 (STP) s^{-1}) at measurement pressure and temperature conditions, and x and y are the mole fractions of component i in the feed and permeate streams, respectively.

The intrinsic selectivity is calculated as the ratio between the permeance of the fast and slow gas components in the feed flowrate, in this case, CO_2 (i) and CH_4 (j) respectively, according to

$$\beta_{ij} = \frac{P_i}{P_j} \tag{4}$$

The mixture separation factor of gas i over gas j, α_{ij}, is defined as the ratio of the relative concentration of the gas components in the permeate and the retentate as [45]

$$\alpha_{ij} = \frac{(y_i/y_j)}{(x_i/x_j)} \tag{5}$$

2.5. Description and validation of the membrane unit model

The experimental results obtained were used as input data for the simulation analysis. A membrane unit programmed in Aspen Custom Modeler was used to determine the desired membrane performance to achieve different targets related to product quality. For this purpose, a crossflow membrane model was developed where a tank-in-series model was applied where the membrane unit was divided into k uniform cells of equal size (with subscript k varying from 1 to n), with the permeate of each cell collected and mixed with the rest of the permeate streams, and the retentate of each cell being the feed of the next [46]. The scheme of the membrane module is illustrated in Fig. 2.

The following hypotheses were considered for the development of the mass transfer model,

- The membrane compaction due to the applied pressure was negligible.
- Transport of gases through the membrane was steady-state, isothermal, and one-dimensional.
- The concentration polarization in the active-side of the membrane module was negligible.
- Permeability was dependent on feed conditions and could be estimated based on the correlation of conditions such as pressure, flow rate and composition [40,47].

Considering these hypotheses, the steady-state material balances were established for determining the changes in gas concentrations and flowrates at both sides of the membrane, as described in our previous work [36]. For the modeling of the gas transport through the membrane layer, the solution-diffusion mechanism was considered, where the driving force of the permeation is the partial pressure difference between permeate and retentate, as shown in equation (6) [48], since the water content within the membrane was kept constant during the set of experimental runs over the whole range of feed concentrations [21], thus

$$N_{C,k} = A_k P_c \left(p_r y_{c,k} - p_p x_{c,k}\right) \tag{6}$$

where $N_{c,k}$ is the molar flowrate of each component permeating though the membrane cell k (kmol h^{-1}), A_k (m^2) is the membrane area of each k cell, P_c is the permeance for each c component across the membrane in

Table 1
Thickness, water uptake and swelling degree of the ILCS/PES- based membranes prepared in this work. CO_2 permeability and intrinsic selectivity, calculated by equation (4) are also included for comparison.

Membrane overlayer	Thickness (μm)	WU (%)	SD (%)	P (CO_2) (Barrer)	β(CO_2/CH_4)
ILCS [36]	12 ± 4	49.0	64.0	154.3	4.3
5 wt% AM-4:ILCS	56 ± 6	80.3	4.26	98.06	26
10 wt% AM-4:ILCS	53 ± 4	88.7	9.19	647.7	6.0
5 wt% ETS-10:ILCS	58 ± 5	67.4	11.58	389.5	30
10 wt% ETS-10:ILCS	74 ± 5	35.2	7.77	135.7	14
5 wt% Zeolite-A:ILCS	75 ± 5	51.9	8.70	779.7	20
10 wt% Zeolite-A:ILCS	62 ± 8	51.72	8.76	419.6	13.0

molar basis (kmol h^{-1} bar^{-1} m^{-2}, that was obtained by the experimental permeance in unit of m^3 (STP) h^{-1} bar^{-1} m^{-2}), x_c and y_c are the molar fraction of each component in the mixture present in the retentate and permeate stream, and p_r and p_p are the pressure on the retentate and permeate sides of the membrane, respectively.

The stage-cut, θ, one of the main parameters used for comparing the membrane performance and predicting the feasibility of scaling-up of the process, is determined as the ratio between the permeate and feed flow rates, as

$$\theta = \frac{F_p}{F_f} \tag{7}$$

The target variables that determine the effectiveness of the membrane in the CO_2/CH_4 separation process are the purity and recovery of the desired components in each stream, given by equations (8) and (9), respectively,

$$Purity_c(\%) = \frac{F_{c,out}}{F_{out}} \times 100 = \frac{F_{out} \times y_{c,out}}{F_{out}} \times 100 = 100 \times y_{c,out} \tag{8}$$

$$Recovery_c(\%) = 100 \times \frac{F_{c,out}}{F_{c,in}} = 100 \times \frac{F_{out} \cdot y_{c,out}}{F_{in} \cdot x_{c,in}} \tag{9}$$

These variables allow determining the quality of the different product streams, so all the specifications must be directed to achieve the maximum purity and recovery of the most permeable component in the permeate and the slowest component in the retentate. Commonly reported targets are set up as a recovery and purity of CO_2 in the permeate side up to 90% and up to 95% for the CH_4 in the retentate side [49]. Due to the difficulty of maximizing both parameters of the process simultaneously, it is necessary to propose a multi-objective task to set both goals at the same time. Finally, another issue that had to be addressed before running the simulations was the number of cells, and its selection must consider the balance between the precision of the model and its calculation load. The cross-flow membrane model implemented in this work for the simulation of the performance of each membrane unit was based in the custom model developed in a prior work for CO_2/CH_4 separation using membrane technology, where the best fitting results were obtained at n = 100 [40]. Considering the previous validation of the developed model with experimental data obtained in the laboratory for a commercial membrane of similar geometry [31], the model is validated further in the present work regarding the mixed gas separation performance of the CS-based composite membranes at varying CO_2 and CH_4 composition in the feed using the same value of n. The deviation between simulated and experimental values at different stage-cut values is estimated by the experimental absolute relative error (AARE) of the target variables to validate the model is estimated by

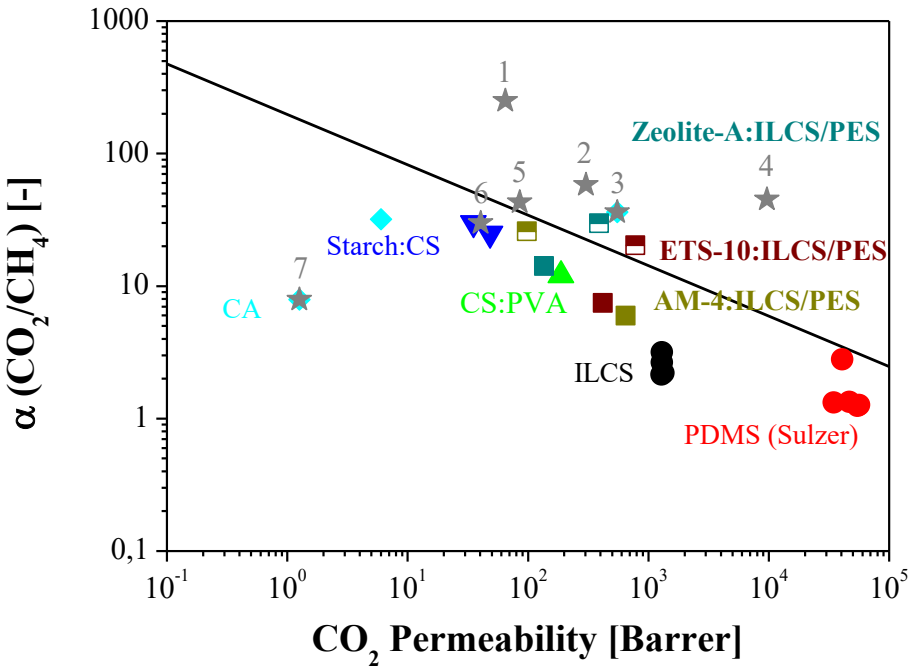

Fig. 3. Comparison of the 5 wt% (half-full squares) and 10 wt% (full squares) filled ILCS/PES membranes prepared in this work and the Robeson upper bound for CO_2/CH_4 separation using polymer membranes. Biopolymer membranes collected by Russo et al. [2] were included for comparison: 1. PLA, 2. PES/PU, 3. ZIF-8/CNF, 4. CNT-PVAm/PVA, 5. PVA/CNC, 6. PVAm/PVA, 7. CA hollow fibres. Starch:CS and CS:PVA are free-standing MMMs prepared in our laboratory in an equimolar basis.

Table 2
Biopolymer based membranes reported for the separation of CO_2/CH_4 mixtures.

Membrane	Characterization	Separation approach	Reference
PVA-g-Starch methacrylate	FTIR, SEM, thermogravimetric analysis (TGA), handling of use	CO_2, N_2 single gas permeability	[15]
Poly(hydroxybutyrate-co-hydroxyvalerate) (PHBV)	Gel permeation chromatography (GPC), SEM, Differential Scanning Calorimetry (DSC), FTIR, solubility of CO_2, toxicity of solvent	CO_2/N_2 and CO_2/CH_4, Flory Huggins model for interaction with the polymer matrix	[8]
Cellulose acetate hollow fibers	FESEM with Electron Dispersion X-ray diffraction EDX,	Separation of CO_2/CH_4	[66,67]
ZIF-62/cellulose acetate	N_2 isotherms, CO_2 adsorption of the fillers, SEM, XRD, morphology, FTIR, TGA (air), Fractional Free Volume (FFV) (from air and ethanol uptake)	Single gas permeation 2–35 bar.Presence of ZIF-62 in the CA matrix improved CO_2 permeation from 15.8 to 84 barrer (*) and selectivity from 12.2 to 35.3	[68]
Cellulose diacetate free standing films	Wide Angle X-ray Diffraction, Atomic Force Microscopy (AFM), gas sorption,	Single gas permeation CO_2, CH_4Effect of film thickness 258 nm to 128 μm	[64]
Bio cellulose acetate (from coconut residue)	SEM, Tensile strength, FTIR, TGA, DSC	Separation of 40:60(v%) CO_2/CH_4 mixtures at 30 °C; thick films of 0.05 mm best performance of separation factor (SF) $(CO_2/CH_4) = 29.56$	[56]
PLA Easy Fil™ -White membrane	DSC, SEM, FTIR	CO_2/CH_4 separation at room temperature. Ideal selectivity of $CO_2/CH_4 = 285$ attained at a CO_2 permeability of 70 barrer.	[12]
Polyurethane/PES	XRD, DSC, TGA, SEM, solution viscosity, porosity (water uptake), mechanical properties (ASTM D638), pressure decay sorption	Separation of CO_2/CH_4. Single gas permeation	[20]
Sodium alginate and sodium carboxymethylcellulose modification of Pebax/PES membranes	FESEM, XRD, TGA-DTG-DSC,	Single gas permeation of CO_2 and CH_4 at 4–7 bar.The presence of biopolymers increased CO_2 permeability from 21 to 35 and 52 barrer, and the ideal selectivity from 22 to 31 and 47.	[22]
CS: silk fibroin (SF) facilitated transport membrane	FESEM, AFM, WCA, RH (%) and swelling degree (SD) (%) in water and glycerol. DMA, TGA (active layer, N_2)	CO_2/N_2 and CO_2/H_2.The optimum CO_2 permeance of 150 GPU (**) and CO_2/N_2 selectivity of 103 for binary gas observed at 90 °C and 0.05 mL/min sweep water flow rate.	[18,23]
Graphene/CS:SF	AFM, FESEM-EDX, TGA, XPS at different temperatures	CO_2, N_2, H_2, gas permeation as a function of water sweep flowrate, temperature and absolute pressure.	[63]
ZIF-8-gC_3N_4/CS	SEM, XRD, TGA, FTIR, ^{13}C NMR, laser particle analyzer	50:50 v/v% CO_2/CH_4 mixed gas permeation experiments.	[32]
(CS + PEG)/PVTMS composite membranes	ATR-FTIR, TGA (N_2), HR-SEM	CO_2, N_2, CH_4 pure gas permeation.P(CO_2) = 153 Barrer, CO_2/CH_4 selectivity = 23	[26]

(*) 1 barrer (unit of intrinsic permeability) = 10^{-10} cm^3(STP) cm cm^{-2} s^{-1} $cmHg^{-1}$.
(**) 1 GPU (gas permeation unit) = 10^{-6} cm^3(STP) cm^{-2} s^{-1} cmHg.

$$AARE(\%) = 100 \times \left| \frac{Simulated\ value - Experimental\ value}{Experimental\ value} \right| \quad (10)$$

3. Results and discussion

3.1. Membranes characterization

The membranes were first characterized regarding their water swelling degree and permeation performance considering the mixed gas permeation experiments at 50:50 (v/v%). Table 1 collects the values of the active layer thickness, water uptake, swelling degree and permeability and intrinsic selectivity data of the membranes. It is worth observing that the most hydrophilic membrane is the 10 wt% AM-4 layered titanosilicate filled composite membrane, offering large permeability at the expense of selectivity. This is attributed to the different morphologies, textural properties and CO_2 adsorption capacities of the particles dispersed in the ILCS matrix of the coated membrane layer, from the 2D AM-4 nanoporous sheets with 9.9 mg CO_2/g uptake [43] to 50 mg CO_2/g of the zeolite 4A [37] and 78 mg CO_2/g of ETS-10 [50]. Liu et al. recently observed that the 2D GO sheets obtained by ionic assembling the GO nanosheets would tune up the CO_2 uptake by increasing surface area [51]. However, 2D fillers providing barrier and selectivity effects are reported at low loadings and they do not benefit by increasing loading in the polymeric matrix, where the high aspect area/volume ratio can lead to cluster agglomerations and defects deteriorating membrane separation performance[52,53].

The intrinsic permeability and selectivity values obtained from the 50:50 (v/v%) CO_2:CH_4 mixed gas separation experiments are also shown in Table1. Here, we can appreciate that CO_2 permeability increased for the 3D ETS-10 and zeolite filled membranes, at a 5 wt% loading, and decreased for lamellar AM-4 at a 5 wt% loading. This can be attributed to the different hydrophilic, swelling as well as CO_2 uptake properties of the selective layer of the membranes as a function of each type of filler. The CO_2/CH_4 separation properties deteriorates as mentioned earlier with increasing loading of lamellar AM-4 titanosilicate [43,54]. This was also observed for the ETS-10 and zeolite A-filled membranes, at a lower magnitude: the CO_2 permeability and CO_2/CH_4 selectivity decreased slightly with increasing ETS-10 titanosilicate loading, despite the synergic hydrophilic and compatibility properties of the titanosilicate and the CS biopolymer reported earlier and enhanced by the IL [28], and less significantly varying with increasing zeolite A loading, which may account for the good compatibility and dispersion of this small-pore zeolite A in the polymer matrix [37].

The swelling degree was calculated by equation (1) to give evidence of the membrane mechanical integrity of the selective ILCS layer. In Table 1, it can be observed how the swelling degree of the 10 wt% AM-4-filled membranes was higher than the 5 wt% AM-4 filled ILCS composite membranes. The increasing loading of hydrophilic AM-4 layered titanosilicate particles caused detachment of the CS-based membrane layer from the substrate underneath leading to higher flux and lower separation factor along experimental runs [55]. This may be attributed to the different aspect ratio influencing adhesion and dispersion of fillers in the CS biopolymer matrix, observed in previous works upon self-standing flat sheet membranes characterization [28,54].

The permeability and selectivity values in Table 1 are plotted in Fig. 3 against the Robeson upper bound to be compared with the state-of-the-art biopolymers reported so far. For this comparison, other biopolymer-based membranes data collected by Russo et al.[2], were included in Fig. 3. We can observe that the 5 wt%-filled ILCS/PES membranes studied in our laboratory were very close to the state-of-the-art of current research for CO_2/CH_4 separation, even overcoming the Robeson upper bound in the case of Zeolite A/ILCS and ETS-10/ILCS

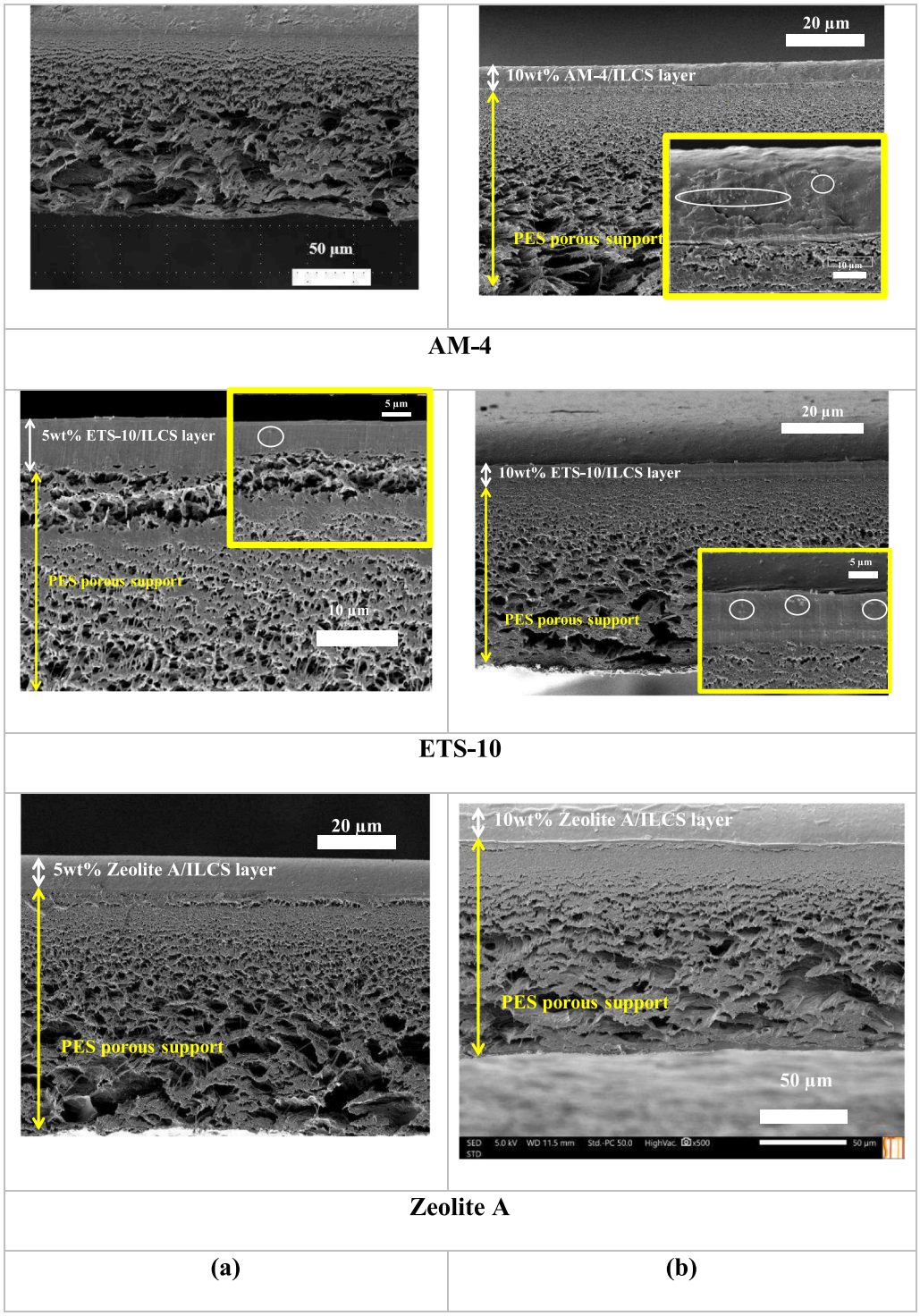

Fig. 4. SEM images of the cross-section of the 5%-filled (a) and 10%-filled (b) ILCS/PES membranes.

composite membranes. The permeability-selectivity trade-off decreases when the inorganic filler loading was increased to 10%. From the experimental separation data in Table 2 plotted in Fig. 3, we observe that the IL-CS/PES mixed matrix composite membranes prepared in this study provided CO_2 permeability and CO_2/CH_4 separation performance in the range acceptable for CO_2/CH_4 separation applications and other biopolymer based mixed matrix membranes recently reported. For instance, a ZIF-8-gC_3N_4/CS membrane with a CO_2 permeability of 153 Barrer and a CO_2/CH_4 selectivity of 24 has been accepted before [32]. Likewise, self-standing, unsupported but 0.05 mm-thick, bio-cellulose acetate membranes were reported to have a CO_2 permeability of 293 Barrer and a CO_2/CH_4 selectivity of 29.5 [56]. In this work, we can affirm that the direct addition of 5 wt% compatible filler loading increased the CO_2/CH_4 selectivity and CO_2 permeability of the unloaded ILCS/PES membranes. This is going to be analyzed upon observing the dispersion of the fillers in the coated membrane layer by EIS and SEM below.

The SEM cross-sectional images shown in Fig. 4 allow verifying the dispersion of the selected fillers on the selective coated top layer, more evident at the higher filler loading of 10 wt% in ILCS. As expected from

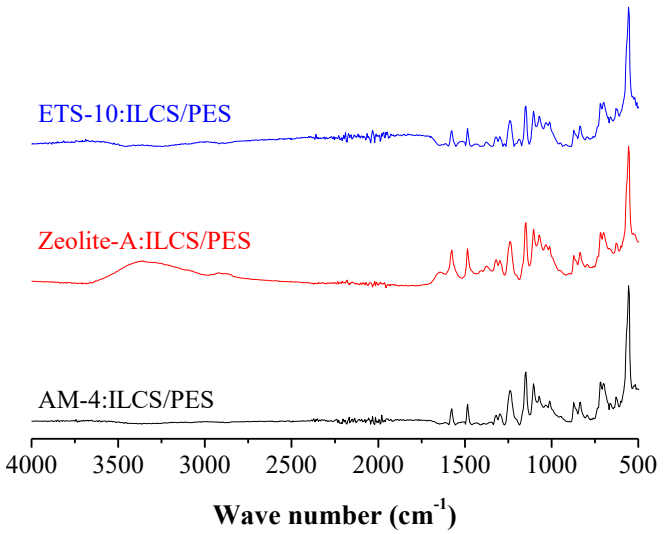

Fig. 5. ATR-FTIR spectra of the prepared 5 wt% loaded ILCS-based mixed matrix composite membranes.

the hydrophilic and swelling properties in Table 1, when the lamellar AM-4 titanosilicate was used as inorganic filler, cluster aglomerations were formed in the membrane matrix, as well as the detachment observed at 10 wt% loading, between the coated CS-based layer and the porous PES substrate, accounting for the deterioration of separation the separation ability of the 10 wt% AM-4/ILCS composite membranes (Table 1 and Fig. 3).

On the other hand, the selective layer thickness observed by SEM presents lower values than those of the freshly made composite membranes, except for 5 wt% AM-4/ILCS composite membrane. Apparently the ETS-10 and zeolite A filled membranes experienced some compaction after all the separation runs, which might be also explaining their increase in selectivity as with polymers with high fractional free volume [57]. CS biopolymer-based membranes show free volume in water-swollen state, and this can be recovered once dried, just by wetting the membranes again, in batch or continuous mode [25,28].

ATR-FTIR is a characterization technique that allows gaining knowledge of the physicochemical characterization properties of the surface as well as the functional groups present on the top layer of a composite membrane. Fig. 5 represents the ATR-FTIR spectra of the 5 wt % filled membranes. The spectra were measured after gas separation experiments. No large differences were observed as a function of the type of filler embedded in the ILCS coated selective layer of the membrane (region 950 – 700 cm^{-1}). This verifies again that the interaction between the Na^{+}-ion exchangeable selected filler and the ILCS matrix is generally good, as observed in the SEM images. The characteristic OH band corresponding to the presence of structural water in the polymer matrix, is present in the region of 3800–3000 cm^{-1}, which confirmed the water uptake (WU) in Table 1 are maintained during gas separation experiments. The bands between 1700 and 600 cm^{-1} are correlated to the presence of the IL in the structure [29]. The ATR-FTIR spectra of the 10 wt% filled membranes were similar and so they are not included in Fig. 5 for clarification.

The EIS analyses provide insight for predicting the diffusion resistance of the coated ion exchange membrane layers overcoming the influence of the porous substrate [58]. The equivalent circuit used for the *Z* fit of Nyquist plots was CP_1-|R_2-CPE_2|-CPE_3 as described in a previous work [59], where CPE_1 and CPE_3 correspond to the capacitance of the double layer at the interfaces PES support/electrode and the CS based membrane/electrode, respectively; CPE_2 corresponds the bulk membrane-PES capacitance and R_2 corresponds to the bulk membrane-PES resistance. We assume that at high frequencies the double layer by hydroxyl ions traveling to/from the interface is negligible or small [59].

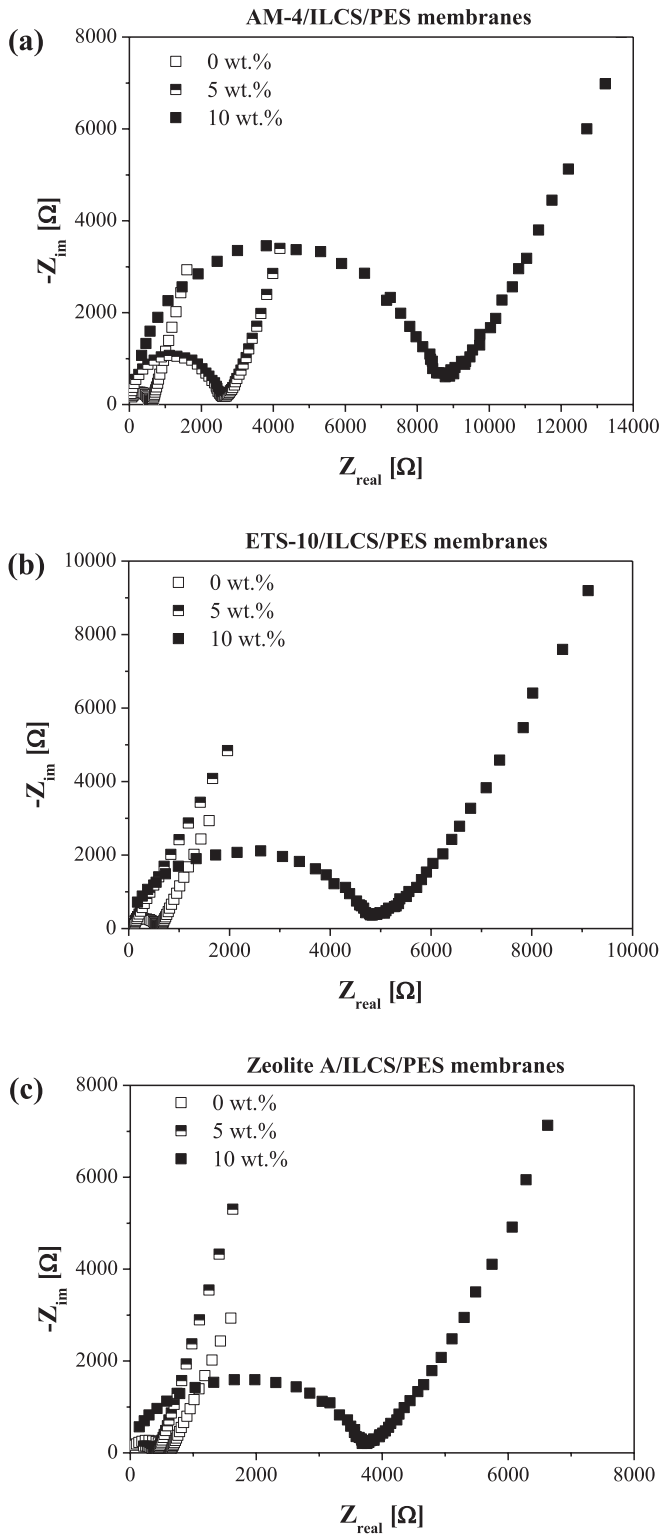

Fig. 6. Experimental data and fitting of the impedance plots of the mixed matrix composite membranes as a function of the amount loading and type of filler: (a) AM-4, (b) ETS-10, and (c) Zeolite A. Measurements were performed in triplicate.

The plots of the mixed matrix composite membranes show a feature similar to ionic conductive materials [60]. The fitting of the figures of merit is shown in Fig. 6 was very accurate. The resistances of ILCS based composite membranes were obtained from the fitting of the above equivalent circuit for the determination of R_2. The resistances given by

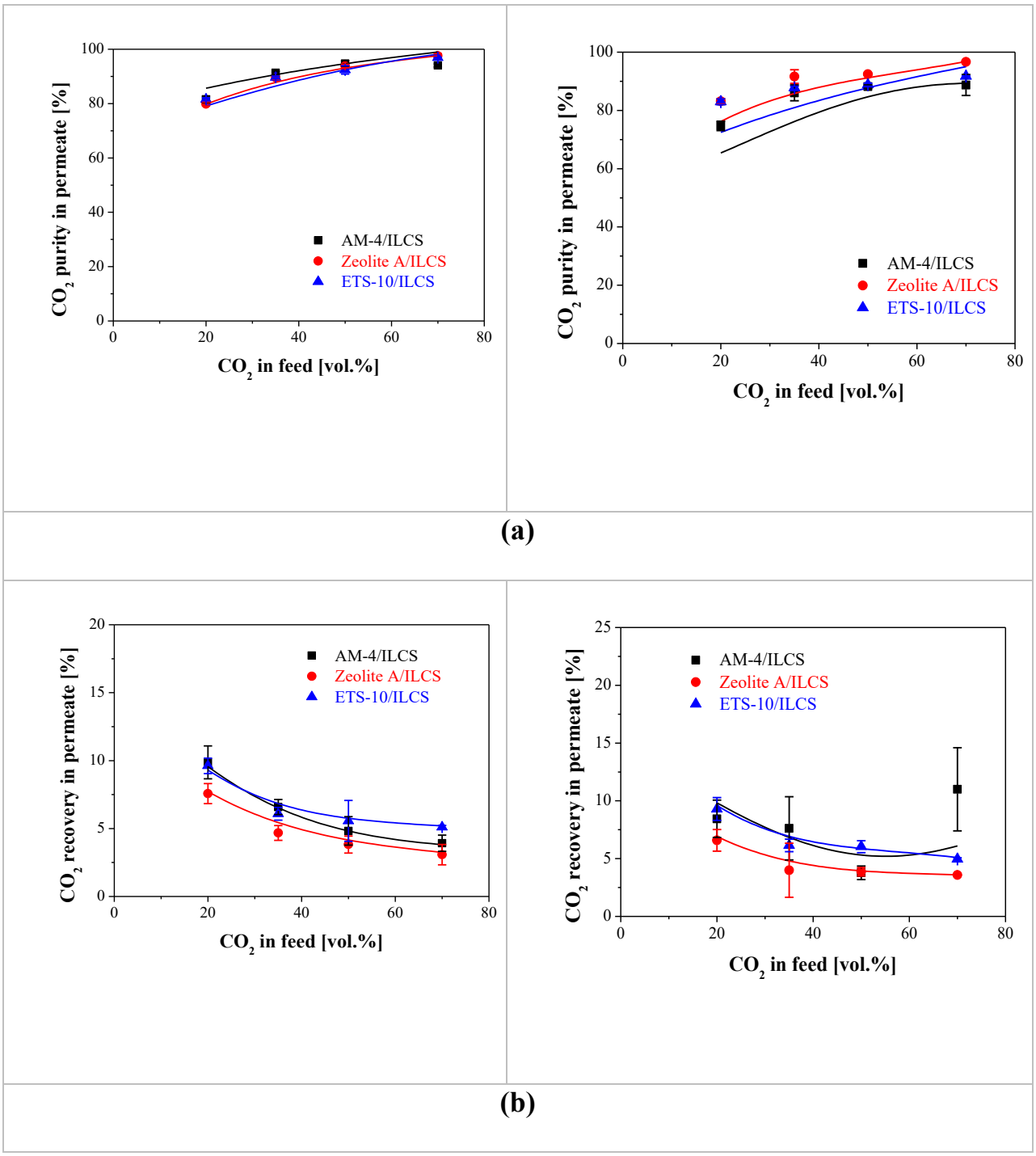

Fig. 7. Purity of CO_2 (a) in the permeate stream for the 5 wt%-filled (left) and 10 wt% (right) ILCS/PES membranes, and recovery of CO_2 in the permeate (b) for the 5 wt%-filled (left) and 10 wt% (right) ILCS/PES membranes, respectively. Lines represent the model simulation. Dots represent the average experimental values in steady-state.

these fittings were 2450, 72 and 410 Ω for the AM-4, ETS-10 and Zeolite A with 5 wt% loading, respectively. It may be of notice that the resistance of the TMC-untreated PES support accounts for only 16 Ω, while the TMC-treated PES support offers a resistance of 70 Ω, so it does significantly contribute to the intrinsic membrane resistance. Furthermore, the ILCS/PES membrane only accounted for a bulk membrane resistance of 550 Ω. The increasing resistance observed in AM-4, ETS-10 and Zeolite A-filled membrane at 10 wt% loading is correlated with the extent of detachment of the coated layer from the porous PES support observed in Fig. 4, which led to higher CO_2 and CH_4 permeance and thus, lower selectivity, due to some clustering of particles in the selective membrane layer matrix upon increasing filler loading, commented above. Using the wet thickness of the freshly activated membranes filled with 5 wt% AM-4, ETS-10 and Zeolite A, the ionic conductivity has values of $9.34 \cdot 10^{-4}$, 0.047 and 0.00409 mS/cm, respectively. Those values are higher than those previously measured for ILCS based membranes without the modified PES support [59,60]. It is remarkable the higher ionic conductivity of the ETS-10 and zeolite A/ILCS composite membranes than those of the laminar titanosilicate filled membranes. Zeolite A is a small pore zeolite with breathable water and CO_2

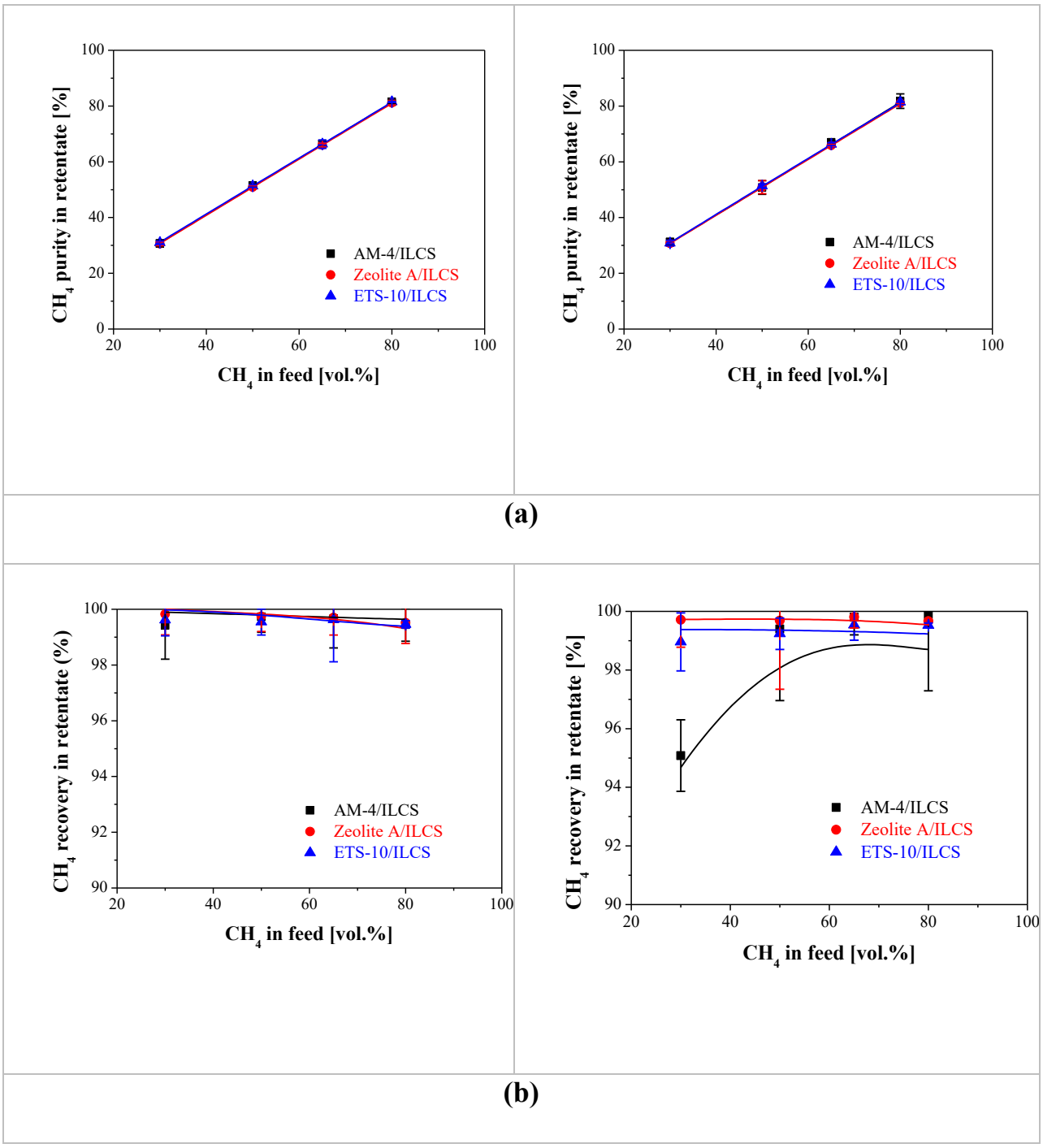

Fig. 8. Purity of CH_4 in the retentate (a) for the 5 wt%-filled (left) and 10 wt% (right) ILCS/PES membranes, and recovery of CH_4 in the retentate (b) for the 5 wt %-filled (left) and 10 wt% (right) ILCS/PES membranes, respectively. Lines represent the model simulation. Dots represent the average experimental values in steady-state.

affinity of its own that is interacting closely with the CS matrix even at 10 wt% loading. The zeolite A into poly(trimethyl-1-silyl-propyne) allowed thus increasing both CO_2 permeability and CO_2/CH_4 selectivity in the presence of relative humidity in the feed stream [37]. Likewise, the titanosilicate-filled membranes provided a lower resistance to the ETS-10 membrane than the AM-4 filled membranes, which can be related to the differences in hydrophilicity observed in Table 1. In addition, these resistances increased with increasing filler loading of all three fillers (with values of 8260, 4860 and 3640 Ω, for the AM-4, ETS-10 and Zeolite A, respectively) in the selective membrane matrix.

For comparison, a summary of the current state-of-the-art of biopolymer-based membranes, including fabrication and characterization, for CO_2/CH_4 separation has been carried out and reviewed in Table 2. The use of characterization techniques like X-ray photoelectron spectroscopy (XPS) employed to characterize water and ion transport in ion exchange membranes have revealed the layer formations within the active membrane matrix and the compatibility with the support by correlating diffusion impedances and transport resistances with varying layer thicknesses [58,61,62]. For example, Prasad et al. used XPS to validate the qualitative and quantitative nature of the chemical

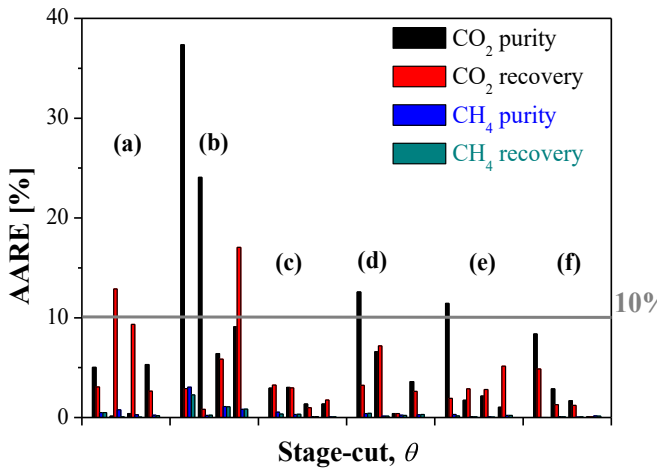

Fig. 9. AARE of the purity and recovery of CO_2 in the permeate and CH_4 in the retentate as a function of stage-cut, for the (a) 5 wt% AM-4/IL-CS, (b) 10 wt% AM-4/ILCS, (c) 5%ETS-10/IL-CS, (d) 10 wt% ETS-10/ILCS, (e) 5 wt% zeolite A/ILCS and (f) 10 wt% Zeolite A/ILCS mixed matrix composite membranes.

structure of graphene/chitosan MMM during CO_2 separation performance [63]. Nguyen et al. correlated the CO_2 and CH_4 transport through cellulose diacetate membranes with crystallinity and membrane thickness by a semi-empiric equation [64], which is instrumental in the development of industrial asymmetric membranes. Besides, these design and fabrication challenges are tuned up by the MMM approach highly explored for conventional polymers, consisting on blending them with other biopolymers or hybridizing with small amount of organic or inorganic fillers [27,52,65] and coating on a compatible porous support [32,55]. The main issue in mixed matrix or composite membranes are a good adhesion or compatibility between the components and the support determining the producibility, selectivity and stability performance [17,39,41].

These techniques can be added to the common selection of analytical techniques reported usually in the synthesis and characterization of membranes for CO_2/CH_4 separation.

3.2. Membrane unit separation performance validation

The CO_2/CH_4 separation performance of the mixed matrix composite membranes with different filler type and loading in the selective layer was validated in the range from 20 vol% to 70 vol% in CO_2 and from 80 vol% to 30 vol% in CH_4, in order to evaluate the behavior of the membranes in different target situations for CO_2 and CH_4 simultaneous recovery. From the experimental results on CO_2 and CH_4 permeance, the target variables purity and recovery of CO_2 and CH_4 in permeate and retentate streams, respectively, were calculated using equations (8) and (9). Fig. 7 collects the CO_2 purity and recovery for the 5 wt% (left) and 10 wt% (right) filled membranes in the permeate, whereas the CH_4 purity and recovery of these membranes is represented in Fig. 8. Please refer to the supporting information for the detailed tables of experimental performance results.

The CO_2 purity in the permeate lied between 80 and 99% for all the membranes in the whole concentration range under study, which stands for the CO_2 selective character of the ILCS-based coated layer [38], but the CO_2 recovery in the permeate stream was low. This is attributed to the low values of experimental stage-cut in the laboratory scale experiments (0.02 – 0.05), which implies a significant increase mainly in two variables: (i) the CO_2 purity in the permeate stream, and (ii) the CH_4 recovery in the retentate stream. To increase more significantly the CO_2 recovery in the permeate, and the CH_4 purity in the retentate streams, higher stage-cuts would be required. The recovery values obtained for the zeolite A/ILCS- are lower than those of the ETS-10/ILCS composite membranes, and the CO_2 recovery of the AM-4/ILCS membrane lies in between. This observation agrees with the ionic and hydrophilic character of the selective layers discussed above. The trend is reverse upon increasing filler loading (Fig. 7(right)) where the appearance of non-idealities in the interface between the high-aspect ratio AM-4 titanosilicate filler and the ILCS matrix is observed and not when ETS-10 nanoparticles were used as filler. The slightly higher CO_2 purity obtained for the zeolite A/ILCS composite membrane confirms as well the role of the water and CO_2 adsorptive cavities of the small pore hydrated zeolite [37].

For the process scaling-up, higher values of stage-cut would be necessary in order to attend to the purity and recovery of both components simultaneously, although higher values of stage-cut also imply higher membrane area requirements (therefore, higher costs). The process optimization would focus on these issues, as these results gave a clear idea on the balance between the different objectives to be covered for the techno-economic optimization of the membrane separation process.

Nevertheless, those CO_2 purity and recovery in the permeate led to a linear increase of the CH_4 purity and high values of CH_4 recovery (greater than 99.01%) in the retentate stream, as observed in Fig. 8. The membrane material did not apparently influence the CH_4 purity and recovery in the retentate stream. This is probably due to the small amount of filler loading (5 wt%) in the bulk of the ILCS/PES membrane configuration. This is confirmed by the CH_4 recovery in the retentate obtained for the 10 wt% filled membranes, where the ETS-10 and zeolite A-based membranes behaved similarly while layered AM-4 filled membrane attained slightly lower values, in agreement with their intrinsic hydrophilic, ionic character and differential morphology, as discussed above.

Other observations derived from Fig. 7 and Fig. 8 is that the agreement of the experimental and simulated purity and recovery values for the 5 wt% loaded mixed matrix composite membranes is generally very close, with relative errors lower than 10% (AARE), especially when the ETS-10 or the zeolite A were used as fillers of the ILCS matrix. As expected, the CO_2 purity of the 10 wt% AM-4/ILCS composite membrane deviates from the experimentally observed value at low CO_2 concentration in the feed. This can be attributed to the higher water uptake and swelling degrees (Table 1) imparted by the high aspect ratio lamellar AM-4 filler than the other 3-dimensional ETS-10 and zeolite A filler particles used in this work. The lamellar AM-4 particles thus provide a lower permeance and stage-cut at 5 wt% loading, while the cluster aggregating and layer detachment observed at increasing filler loading deteriorated the separation properties of the AM-4/ILCS composite membranes at 10 wt%. Usually, layered materials are filled in at low loadings in the mixed matrix membranes because of the high-aspect ratio providing contact with the polymer matrix and the diminished particle size upon exfoliation of the nanosheets leading to agglomeration at higher loadings [53,69].

Fig. 9 collects the deviation between simulated and experimental CO_2 and CH_4 purity and recovery in the permeate and retentate streams, calculated by equation (10). As expected, only the AM-4 filled mixed matrix composite membrane surpassed values of AARE larger than 10%, due to the lower flux and stage-cut conducing to higher sensitivity than the other membranes tested in this work. Please refer to the Supporting information for the full recollection of CO_2 and CH_4 purity and recovery values and their AARE in both streams.

4. Conclusions

This work validates the mixed gas separation performance of novel chitosan-based composite membranes for CO_2/CH_4 separation in a whole range of feed concentrations, to evaluate the potential in different applications. Mixed matrix composite membranes were prepared by hybridizing chitosan biopolymer solution with a 5 wt% [emim][acetate] (IL) and 5, 10 wt% loading of Na^+-exchangeable fillers in different

morphologies and compositions, as layered AM-4 titanosilicate, 3D ETS-10 titanosilicate and small-pore zeolite 4A, influencing in their CO_2 permeance and CO_2/CH_4 separation factor. The membranes were characterized regarding their water uptake and swelling, film thickness and physicochemical properties of the coated layer. The membranes were used to validate a previously developed cross-flow mathematical model focusing in two target objectives, the purity and recovery of permeate and retentate simultaneously. The CO_2 purity in the permeate was highly dependent on the composition, dispersion, and adhesion of the selective membrane layer components among them and with the porous PES support.

Further work is being performed regarding the optimization and techno-economic assessment of the best CS- based composite membranes to maximize both CO_2 and CH_4 recovery in the permeate and retentate streams, that is, the 5 wt% ETS-10 and zeolite A filled ILCS-based mixed matrix composite membranes studied in this work. The effect of thickness and blending with other biopolymers with higher intrinsic permeability on membrane and process configuration are also being undertaken in a future work.

Declaration of Competing Interest

The authors declare that they have no known competing financial interests or personal relationships that could have appeared to influence the work reported in this paper.

Data availability

Data will be made available on request.

Acknowledgements

This research was funded by the Spanish Ministry for Science and Innovation, grant numbers PID2019-108136RB-C31 and PID2019-108136RB-C32 of the Spanish Research Agency (AEI/10.13039/501100011033). A.T.C. also acknowledges the Ministry for the Early-Stage researcher contract (FPI grant no. PRE2020-09765/AEI/10.13039/501100011033) and the Scientific Committee of the International Separation and Purification Technology Congress (ISPT 2022, Elsevier) celebrated online in December 2022 for the Best Poster Award. Alba Pérez Cañaveras and the General Analytical Services at the University of Alicante are also gratefully acknowledged.

Appendix A. Supplementary data

Supplementary data to this article can be found online at https://doi.org/10.1016/j.seppur.2023.124535.

References

[1] U. Brémond, A. Bertrandias, J.P. Steyer, N. Bernet, H. Carrere, A vision of European biogas sector development towards 2030: Trends and challenges, J. Clean. Prod. 287 (2021) 125065, https://doi.org/10.1016/j.jclepro.2020.125065.
[2] F. Russo, F. Galiano, A. Iulianelli, A. Basile, A. Figoli, Biopolymers for sustainable membranes in CO_2 separation: a review, Fuel Process. Technol. 213 (2021) 106643, https://doi.org/10.1016/j.fuproc.2020.106643.
[3] R. Borgohain, U. Pattnaik, B. Prasad, B. Mandal, A review on chitosan-based membranes for sustainable CO2 separation applications: Mechanism, issues, and the way forward, Carbohydr. Polym. 267 (2021) 118178, https://doi.org/10.1016/j.carbpol.2021.118178.
[4] V. Vatanpour, M.E. Pasaoglu, H. Barzegar, O.O. Teber, R. Kaya, M. Bastug, A. Khataee, I. Koyuncu, Cellulose acetate in fabrication of polymeric membranes: A review, Chemosphere 295 (2022) 133914, https://doi.org/10.1016/j.chemosphere.2022.133914.
[5] V. Vatanpour, B. Yavuzturk Gul, B. Zeytuncu, S. Korkut, G. İlyasoğlu, T. Turken, M. Badawi, I. Koyuncu, M.R. Saeb, Polysaccharides in fabrication of membranes: A review, Carbohydr. Polym. 281 (2022), https://doi.org/10.1016/j.carbpol.2021.119041.
[6] X. Dong, D. Lu, T.A.L. Harris, I.C. Escobar, Polymers and solvents used in membrane fabrication: A review focusing on sustainable membrane development, Membranes (Basel). 11 (2021) 309–334, https://doi.org/10.3390/membranes11050309.
[7] P. López-Porfiri, P. Gorgojo, M. Gonzalez-Miquel, Green solvent selection guide for biobased organic acid recovery, ACS Sustain. Chem. Eng. 8 (2020) 8958–8969, https://doi.org/10.1021/acssuschemeng.0c01456.
[8] K. Papchenko, M. Degli Esposti, M. Minelli, P. Fabbri, D. Morselli, M.g., De Angelis, New sustainable routes for gas separation membranes: The properties of poly (hydroxybutyrate-co-hydroxyvalerate) cast from green solvents, J. Memb. Sci. 660 (2022) 120847, https://doi.org/10.1016/j.memsci.2022.120847.
[9] F. Galiano, K. Briceño, T. Marino, A. Molino, K.V. Christensen, A. Figoli, Advances in biopolymer-based membrane preparation and applications, J. Memb. Sci. 564 (2018) 562–586, https://doi.org/10.1016/j.memsci.2018.07.059.
[10] C. Cottet, Y.A. Ramirez-Tapias, J.F. Delgado, O. de la Osa, A.G. Salvay, M. A. Peltzer, Biobased materials from microbial biomass and its derivatives, Materials (Basel). 13 (2020) 1–26.
[11] Z. Dai, J. Deng, Q. Yu, R.M.L. Helberg, S. Janakiram, L. Ansaloni, L. Deng, Fabrication and evaluation of bio-based nanocomposite TFC hollow fiber memranes for enhanced CO_2 capture, ACS Appl. Mater. Interfaces. 11 (2019) 10874–10882, https://doi.org/10.1021/acsami.8b19651.
[12] A. Iulianelli, F. Russo, F. Galiano, G. Desiderio, A. Basile, A. Figoli, PLA Easy Fil – White-based membranes for CO_2 separation, greenh, Gases Sci. Technol. 9 (2019) 360–369, https://doi.org/10.1002/ghg.1853.
[13] Y. Qin, X. Sheng, S. Liu, G. Ren, X. Wang, F. Wang, Recent advances in carbon dioxide based copolymers, J. CO_2 Util. 11 (2015) 3–9, https://doi.org/10.1016/j.jcou.2014.10.003.
[14] B. Bolto, T. Tran, M. Hoang, Z. Xie, Crosslinked poly(vinyl alcohol) membranes, Prog. Polym. Sci. 34 (2009) 969–981, https://doi.org/10.1016/j.progpolymsci.2009.05.003.
[15] M. Patil, S.N. Mathad, A.Y. Patil, M.N. Arshad, H.S. Alorfi, M. Puttegowda, A. M. Asiri, A. Khan, N. Azum, Synthesis and characterization of microwave-assisted copolymer membranes of poly(vinyl alcohol)-g-starch methacrylate and their evaluation for gas transport properties, Polymers (Basel). 14 (2022) 350–361, https://doi.org/10.3390/polym14020350.
[16] E.S. Dragan, M.V. Dinu, Advances in porous chitosan-based composite hydrogels: Synthesis and applications, React. Funct. Polym. 146 (2020) 104372, https://doi.org/10.1016/j.reactfunctpolym.2019.104372.
[17] C. Casado-Coterillo, A. Garea, Á. Irabien, Effect of water and organic pollutant in CO_2/CH_4 separation using hydrophilic and hydrophobic composite membranes, Membranes (Basel). 10 (2020) 405–417, https://doi.org/10.3390/membranes10120405.
[18] B. Prasad, B. Mandal, Moisture responsive and CO_2 selective biopolymer membrane containing silk fibroin as a green carrier for facilitated transport of CO_2, J. Memb. Sci. 550 (2018) 416–426, https://doi.org/10.1016/j.memsci.2017.12.061.
[19] R. Borgohain, B. Mandal, Thermally stable and moisture responsive carboxymethyl chitosan/dendrimer/hydrotalcite membrane for CO_2 separation, J. Memb. Sci. 608 (2020) 118214, https://doi.org/10.1016/j.memsci.2020.118214.
[20] S. Saedi, S.S. Madaeni, K. Hassanzadeh, A.A. Shamsabadi, S. Laki, The effect of polyurethane on the structure and performance of PES membrane for separation of carbon dioxide from methane, J. Ind. Eng. Chem. 20 (2014) 1916–1929, https://doi.org/10.1016/j.jiec.2013.09.012.
[21] X. He, D.R. Nieto, A. Lindbråthen, M.-B. Hägg, Membrane system design for CO_2 capture: from molecular modeling to process simulation, in: A.I. Papadopoulos, P. Seferlis (Eds.), Mater. Process Syst. CO_2 Capture Model. Des. Control Integr, 1st ed.,, John Wiley and Sons Ltd., 2017, pp. 249–281, https://doi.org/10.1002/9781119106418.ch10.
[22] S.K. Salestan, A. Rahimpour, R. Abedini, Experimental and theoretical studies of biopolymers on the efficient CO_2/CH_4 separation of thin-film Pebax®1657 membrane, Chem. Eng. Process. - Process Intensif. 163 (2021) 108366, https://doi.org/10.1016/j.cep.2021.108366.
[23] B. Prasad, R.M. Thakur, B. Mandal, B. Su, Enhanced CO_2 separation membrane prepared from waste by-product of silk fibroin, J. Memb. Sci. 587 (2019) 117170, https://doi.org/10.1016/j.memsci.2019.117170.
[24] P. Stanovský, M. Benkocká, Z. Kolská, M. Šimčík, P. Slepička, V. Švorčík, K. Friess, M.C. Ruzicka, P. Izak, Permeability enhancement of chemically modified and grafted polyamide layer of thin-film composite membranes for biogas upgrading, J. Memb. Sci. 641 (2022) 119890, https://doi.org/10.1016/j.memsci.2021.119890.
[25] C. Casado-Coterillo, A. Fernández-Barquín, A. Irabien, Effect of humidity on CO_2/N_2 and CO_2/CH_4 separation using novel robust mixed matrix composite hollow fiber membranes: Experimental and model evaluation, Membranes (Basel). 10 (2020) 6–20, https://doi.org/10.3390/membranes10010006.
[26] S. Kunalan, K. Palanivelu, E.K. Sachin, D.A. Syrtsova, V.V. Teplyakov, Thin-film hydrogel polymer layered polyvinyltrimethylsilane dual-layer flat-bed composite membrane for CO_2 gas separation, J. Appl. Polym. Sci. 139 (2022) e52024.
[27] M. Ahmadi, S. Janakiram, Z. Dai, L. Ansaloni, L. Deng, Performance of mixed matrix membranes containing porous two-dimensional (2D) and three-dimensional (3D) fillers for CO_2 separation: A review, Membranes (Basel). 8 (2018) 50–98, https://doi.org/10.3390/membranes8030050.
[28] C. Casado-Coterillo, M. del Mar López-Guerrero, Á. Irabien, Synthesis and characterisation of ETS-10/acetate-based ionic liquid/chitosan mixed matrix membranes for CO_2/N_2 permeation, Membranes (Basel) 4 (2) (2014) 287–301.
[29] M.D.M. López Guerrero, C. Casado-Coterillo, A. Irabien, Synergistic effect of combining titanosilicate and 1-Ethyl-3-methylimidazolium acetate in mixed matrix membranes for efficient CO_2 separation, EJSD 4 (2) (2015).

[30] Z. Dai, R.D. Noble, D.L. Gin, X. Zhang, L. Deng, Combination of ionic liquids with membrane technology: A new approach for CO_2 separation, J. Memb. Sci. 497 (2016) 1–20, https://doi.org/10.1016/j.memsci.2015.08.060.

[31] H. Xie, S. Zhang, S. Li, Chitin and chitosan dissolved in ionic liquids as reversible sorbents of CO_2, Green Chem. 8 (2006) 630–633, https://doi.org/10.1039/b517297g.

[32] A. Jomekian, B. Bazooyar, J. Esmaeilzadeh, R.M. Behbahani, Highly CO_2 selective chitosan/g-C_3N_4/ZIF-8 membrane on polyethersulfone microporous substrate, Sep. Purif. Technol. 236 (2020) 116307, https://doi.org/10.1016/j.seppur.2019.116307.

[33] Z.V. Singh, M.G. Cowan, W.M. McDanel, Y. Luo, R. Zhou, D.L. Gin, R.D. Noble, Determination and optimization of factors affecting CO_2/CH_4 separation performance in poly(ionic liquid)-ionic liquid-zeolite mixed-matrix membranes, J. Memb. Sci. 509 (2016) 149–155, https://doi.org/10.1016/j.memsci.2016.02.034.

[34] L.M. Robeson, The upper bound revisited, J. Memb. Sci. 320 (2008) 390–400, https://doi.org/10.1016/j.memsci.2008.04.030.

[35] M.P. Rivera, R.P. Lively, Analysis of gas transport in molecularly-mixed composite membranes, J. Memb. Sci. 661 (2022) 120880, https://doi.org/10.1016/j.memsci.2022.120880.

[36] A. Torre-Celeizabal, C. Casado-Coterillo, A. Garea, Biopolymer-based mixed matrix membranes (MMMs) for CO_2/CH_4 separation: Experimental and modeling evaluation, Membranes (Basel). 12 (2022) 561–583, https://doi.org/10.3390/membranes12060561.

[37] A. Fernández-Barquín, R. Rea, D. Venturi, M. Giacinti-Baschetti, M.G. De Angelis, C. Casado-Coterillo, Á. Irabien, Effect of relative humidity on the gas transport properties of zeolite A/PTMSP mixed matrix membranes, RSC Adv. 8 (2018) 3536–3546, https://doi.org/10.1039/c7ra13039b.

[38] E. Santos, E. Rodríguez-Fernández, C. Casado-Coterillo, Á. Irabien, Hybrid ionic liquid-chitosan membranes for CO_2 separation: Mechanical and thermal behavior, Int. J. Chem. React. Eng. 14 (2016) 713–718, https://doi.org/10.1515/ijcre-2014-0109.

[39] A. Fernández-Barquín, C. Casado-Coterillo, M. Etxeberria-Benavides, J. Zuñiga, A. Irabien, Comparison of flat and hollow-fiber mixed-matrix composite membranes for CO_2 separation with temperature, Chem. Eng. Technol. 40 (2017) 997–1007, https://doi.org/10.1002/ceat.201600580.

[40] R. Abejon, C. Casado-Coterillo, A. Garea, Multiobjective optimization based on "Distance-to-Target" approach of membrane units for separation of CO_2/CH_4, Processes. 9 (2021) 1871–1896.

[41] S.S. Madaeini, M.M.S. Badieh, V. Vatanpour, Effect of coating method on gas separation by PDMS/PES membrane, Polym. Eng. Sci. 53 (2013) 1878–1885, https://doi.org/10.1002/pen.23456.

[42] S. Xiao, X. Feng, R.Y.M. Huang, Trimesoyl chloride crosslinked chitosan membranes for CO_2/N_2 separation and pervaporation dehydration of isopropanol, J. Memb. Sci. 306 (2007) 36–46, https://doi.org/10.1016/j.memsci.2007.08.021.

[43] C. Casado, D. Ambroj, Á. Mayoral, E. Vispe, C. Téllez, J. Coronas, Synthesis, swelling, and exfoliation of microporous lamellar titanosilicate AM-4, Eur. J. Inorg. Chem. 4 (2011) 2247–2253, https://doi.org/10.1002/ejic.201100152.

[44] C. Casado, Z. Amghouz, J.R. García, K. Boulahya, J.M. González-Calbet, C. Téllez, J. Coronas, Synthesis and characterization of microporous titanosilicate ETS-10 obtained with different Ti sources, Mater. Res. Bull. 44 (2009) 1225–1231, https://doi.org/10.1016/j.materresbull.2009.01.015.

[45] P. Seghman, L. Krátký, T. Jirout, Selectivity and separation factor for components during multicomponent membrane gas separation, Chem. Eng. Trans. 92 (2022) 109–114, https://doi.org/10.3303/CET2292019.

[46] J. Tao, J. Wang, L. Zhu, X. Chen, Integrated design of multi-stage membrane separation for landfill gas with uncertain feed, J. Memb. Sci. 590 (2019) 117260, https://doi.org/10.1016/j.memsci.2019.117260.

[47] M. Samei, A. Raisi, Multi-stage gas separation process for separation of carbon dioxide from methane: Modeling, simulation, and economic analysis, Chem. Eng. Process. - Process Intensif. 170 (2022) 108676, https://doi.org/10.1016/j.cep.2021.108676.

[48] J.G. Wijmans, R.W. Baker, The solution-diffusion model: A review, J. Memb. Sci. 107 (1-2) (1995) 1–21.

[49] P.F. Zito, A. Brunetti, G. Barbieri, Multi-step membrane process for biogas upgrading, J. Memb. Sci. 652 (2022) 120454, https://doi.org/10.1016/j.memsci.2022.120454.

[50] V. Martin-Gil, A. Lopez, P. Hrabanek, R. Mallada, I.F.J. Vankelecom, V. Fila, Study of different titanosilicate (TS-1 and ETS-10) as fillers for mixed matrix membranes for CO_2/CH_4 gas separation appilcations, J. Memb. Sci. 523 (2017) 24–35, https://doi.org/10.1016/j.memsci.2016.09.041.

[51] Z. Liu, W. Zhang, M. Yin, Y. Ren, Q. An, Ion-crosslinking induced dynamic assembly of porous 3D graphene oxide framework for CO_2 capture, Sep. Purif. Technol. 312 (2023) 123448, https://doi.org/10.1016/j.seppur.2023.123448.

[52] M.M. Zagho, M.K. Hassan, M. Khraisheh, M.A.A. Al-Maadeed, S. Nazarenko, A review on recent advances in CO_2 separation using zeolite and zeolite-like materials as adsorbents and fillers in mixed matrix membranes (MMMs), Chem. Eng. J. Adv. 6 (2021) 100091, https://doi.org/10.1016/j.ceja.2021.100091.

[53] B. Zornoza, P. Gorgojo, C. Casado, C. Téllez, J. Coronas, Mixed matrix membranes for gas separation with special nanoporous fillers, Desalin. Water Treat. 27 (2011) 42–47, https://doi.org/10.5004/dwt.2011.2045.

[54] L. García-Cruz, C. Casado-Coterillo, J. Iniesta, V. Montiel, Á. Irabien, Chitosan: Poly (vinyl) alcohol composite alkaline membrane incorporating organic ionomers and layered silicate materials into a PEM electrochemical reactor, J. Memb. Sci. 498 (2016) 395–407, https://doi.org/10.1016/j.memsci.2015.08.040.

[55] A. Torre-Celeizabal, A. Garea, C. Casado-Coterillo, Chitosan: Polyvinyl alcohol based mixed matrix sustainable coatings for reusing composite membranes in water treatment: Fouling characterization, Chem. Eng. J. Adv. 9 (2022) 100236, https://doi.org/10.1016/j.ceja.2021.100236.

[56] A. Khamwichit, S. Wattanasit, W. Dechapanya, Synthesis of bio-cellulose acetate membranefrom coconut juice residues for carbon dioxide Removal from biogas in membrane unit, Front. Energy Res. 9 (2021), https://doi.org/10.3389/fenrg.2021.670904.

[57] A. Fernández-Barquín, C. Casado-Coterillo, M. Palomino, S. Valencia, A. Irabien, LTA/Poly(1-trimethylsilyl-1-propyne) mixed-matrix membranes for high-temperature CO_2/N_2 separation, Chem. Eng. Technol. 38 (2015) 658–666, https://doi.org/10.1002/ceat.201400641.

[58] V. Freger, S. Bason, Characterization of ion transport in thin films using electrochemical impedance spectroscopy. I. Principles and theory, J. Memb. Sci. 302 (2007) 1–9, https://doi.org/10.1016/j.memsci.2007.06.046.

[59] L. García-Cruz, C. Casado-Coterillo, J. Iniesta, V. Montiel, Á. Irabien, Preparation and characterization of novel chitosan-based mixed matrix membranes resistant in alkaline media, J. Appl. Polym. Sci. 132 (2015) 42240, https://doi.org/10.1002/app.42240.

[60] Y. Xiong, H. Wang, C. Wu, R. Wang, Preparation and characterization of conductive chitosan-ionic liquid composite membranes, Polym. Adv. Technol. 23 (2012) 1429–1434, https://doi.org/10.1002/pat.2061.

[61] S. Bason, A. Ben-David, Y. Oren, V. Freger, Characterization of ion transport in the active layer of RO and NF polyamide membranes, Desalination 199 (2006) 31–33, https://doi.org/10.1016/j.desal.2006.03.137.

[62] V. Freger, Diffusion impedance and equivalent circuit of a multilayer film, Electrochem. Commun. 7 (2005) 957–961, https://doi.org/10.1016/j.elecom.2005.06.020.

[63] B. Prasad, B. Mandal, Graphene-incorporated biopolymeric mixed-matrix membrane for enhanced CO2 separation by regulating the support pore filling, ACS Appl. Mater. Interfaces. 10 (2018) 27810–27820, https://doi.org/10.1021/acsami.8b09377.

[64] H. Nguyen, M. Wang, M.Y. Hsiao, K. Nagai, Y. Ding, H. Lin, Suppression of crystallization in thin films of cellulose diacetate and its effect on CO_2/CH_4 separation properties, J. Memb. Sci. 586 (2019) 7–14, https://doi.org/10.1016/j.memsci.2019.05.039.

[65] M.G. Buonomenna, W. Yave, G. Golemme, Some approaches for high performance polymer based membranes for gas separation: block copolymers, carbon molecular sieves and mixed matrix membranes, RSC Adv. 2 (2012) 10745–10773, https://doi.org/10.1039/c2ra20748f.

[66] M. Mubashir, Y.F. Yeong, K.K. Lau, T.L. Chew, Effect of spinning conditions on the fabrication of cellulose acetate hollow fiber membrane for CO_2 separation from N_2 and CH_4, Polym. Test. 73 (2019) 1–11, https://doi.org/10.1016/j.polymertesting.2018.10.036.

[67] M. Mubashir, Y.F. Yeong, T.L. Chew, K.K. Lau, Optimization of spinning parameters on the fabrication of NH2-MIL-53(Al)/cellulose acetate (CA) hollow fiber mixed matrix membrane for CO_2 separation, Sep. Purif. Technol. 215 (2019) 32–43, https://doi.org/10.1016/j.seppur.2018.12.086.

[68] M. Mubashir, L.F. Dumée, Y.Y. Fong, N. Jusoh, J. Lukose, W.S. Chai, P.L. Show, Cellulose acetate-based membranes by interfacial engineering and integration of ZIF-62 glass nanoparticles for CO_2 separation, J. Hazard. Mater. 415 (2021), https://doi.org/10.1016/j.jhazmat.2021.125639.

[69] A. Jamil, O.P. Ching, A.B.M. Shariff, Current status and future prospect of polymer-layered silicate mixed-matrix membranes for CO_2/CH_4 separation, Chem. Eng. Technol. 39 (2016) 1393–1405, https://doi.org/10.1002/ceat.201500395.